Taylor & Francis
Taylor & Francis Group

Historical Biology
An International Journal of Paleobiology

ISSN: 0891-2963 (Print) 1029-2381 (Online) Journal homepage: http://www.tandfonline.com/loi/ghbi20

A new desmostylian mammal from Unalaska (USA) and the robust Sanjussen jaw from Hokkaido (Japan), with comments on feeding in derived desmostylids

Kentaro Chiba, Anthony R. Fiorillo, Louis L. Jacobs, Yuri Kimura, Yoshitsugu Kobayashi, Naoki Kohno, Yosuke Nishida, Michael J. Polcyn & Kohei Tanaka

To cite this article: Kentaro Chiba, Anthony R. Fiorillo, Louis L. Jacobs, Yuri Kimura, Yoshitsugu Kobayashi, Naoki Kohno, Yosuke Nishida, Michael J. Polcyn & Kohei Tanaka (2016) A new desmostylian mammal from Unalaska (USA) and the robust Sanjussen jaw from Hokkaido (Japan), with comments on feeding in derived desmostylids, Historical Biology, 28:1-2, 289-303, DOI: 10.1080/08912963.2015.1046718

To link to this article: http://dx.doi.org/10.1080/08912963.2015.1046718

Historical Biology, 2016
Vol. 28, Nos. 1–2, 289–303, http://dx.doi.org/10.1080/08912963.2015.1046718

A new desmostylian mammal from Unalaska (USA) and the robust Sanjussen jaw from Hokkaido (Japan), with comments on feeding in derived desmostylids

Kentaro Chiba[a], Anthony R. Fiorillo[b], Louis L. Jacobs[c*], Yuri Kimura[d], Yoshitsugu Kobayashi[e], Naoki Kohno[f], Yosuke Nishida[c], Michael J. Polcyn[c] and Kohei Tanaka[g]

[a]Department of Ecology and Evolutionary Biology, University of Toronto, Toronto, Ontario, Canada, M5S 3B2; [b]Perot Museum of Nature and Science, 2201 North Field Street, Dallas, Texas 75201, USA; [c]Roy M. Huffington Department of Earth Sciences, Southern Methodist University, Dallas, Texas 75275, USA; [d]Department of Geology and Paleontology, National Museum of Nature and Science, 4-1-1 Amakubo Tsukuba, Ibaraki 305-0005, Japan; [e]Hokkaido University Museum, Kita 10, Nishi 8, Kita-Ku, Sapporo, Hokkaido 060-0810, Japan; [f]Department of Geology and Paleontology, National Museum of Nature and Science, and Graduate School of Life and Environmental Sciences, University of Tsukuba, Tsukuba, Japan; [g]Department of Geoscience, University of Calgary, 2500 University Drive NW, Calgary, Alberta, Canada, T2N 1N4

(*Received 30 January 2015; accepted 24 April 2015*)

Derived members of the enigmatic mammalian order Desmostylia have molars comprising appressed columns whose morphology does not render their function in feeding simple to discern. Here we describe a new genus and species, *Ounalashkastylus tomidai*, more derived than *Cornwallius* but less derived than *Desmostylus* and *Vanderhoofius*, which develop a hypertrophied medial eminence on the dentary ontogenetically. Tooth morphology, vaulted palate and the medial eminence, which can rise to the level of the occlusal surface of M_2, suggest that derived desmostylids clenched their teeth strongly while employing suction during feeding, most likely on marine and coastal plants.

Keywords: marine mammal; phylogeny; paleoecology; North Pacific

Introduction

The Order Desmostylia is unique among mammalian orders in being limited in age to the Oligocene and Miocene epochs (33-10 Ma; Barnes 2013), limited in distribution to the North Pacific, and in being the only order of marine mammals to have gone totally extinct (Domning 2001, 2008). The diversity of the order comprises some eight or so genera divided between two families, the Paleoparadoxiidae and Desmostylidae (Domning 2008; Beatty 2009; Barnes 2013). Desmostylians were coastal marine, forelimb-dominated swimmers (Domning 2002; Gingerich 2005; Hayashi et al. 2013). They are considered herbivores (Clementz et al. 2003; Domning and Pyenson 2008; Barnes 2013), but derived desmostylids have unique cheek teeth comprising an unusually large number of closely appressed, columnar cusps that wear into rings of enamel surrounding a dentine core. The teeth do not lend themselves readily to functional and dietary interpretation because, while the enamel rings show wear and polish, they have not revealed consistent patterns related to habitual chewing motions as in other primitive or derived tribosphenic mammals.

Here we describe a new genus and species of desmostylid from the Aleutian island of Unalaska (Figure 1) and provide a phylogenetic analysis showing it is more derived than *Cornwallius* in having added columns to the molars, but more basal than *Desmostylus* in being lower crowned and lacking a hypertrophied medial eminence on the dentary. In addition, we use a large dentary referred to cf. *Vanderhoofius* sp. from the Sanjussen River, Hokkaido, Japan (Figure 1), as a platform to investigate the ontogenetic variation of the medial eminence in derived desmostylids and conjecture its role in desmostylian feeding.

Materials and methods

As part of a paleontological reconnaissance project funded by the US National Park Service, Alaska Regional Office, ARF and LLJ visited the island of Unalaska in 2004 to investigate United States Geological Survey reports of a desmostylian from the Dutch Harbor member of the Unalaska Formation (Jacobs et al. 2007). The specimens from Unalaska used in this study were recovered during earlier quarry operations, on which a school is now built within the city of Unalaska. After a public lecture by ARF at the Museum of the Aleutians in Unalaska that year prior to fieldwork, the specimens were offered to ARF and LLJ for study.

The Sanjussen specimen was discovered by Dr. Nachio Minoura of Hokkaido University and his students in 2000. It was scanned with a General Electric Lightspeed Ultra Multislice CT scanner with an inter-slice spacing of 0.1 mm (312 kV, 204 mA) at the National Museum of

---

*Corresponding author. Email: jacobs@mail.smu.edu

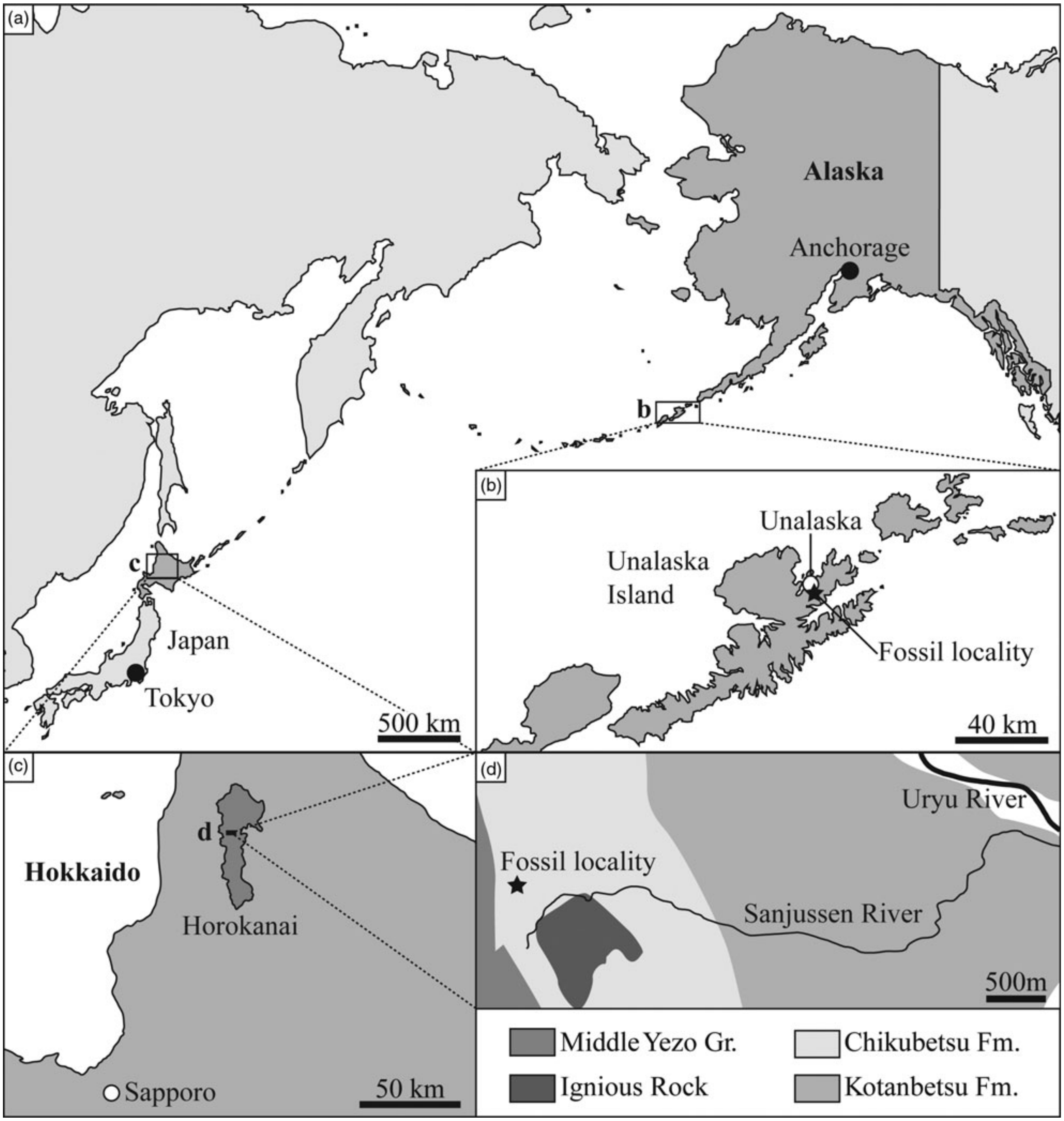

Figure 1. Location map of desmostylid specimens described in this study (a) overview, (b) *Ounalashkastylus tomidai* locality on Unalaska Island, Alaska, USA and (c,d) locality of cf. *Vanderhoofius* sp. along the Sanjussen River, Hokkaido, Japan.

Nature and Science, Tokyo, to examine and evaluate the bony medial eminence of the dentary. Our specific purpose in CT scanning this specimen was to determine whether the medial eminence might be pathological.

In order to visualise the characters we describe, three-dimensional (3-D) surface scans of specimens used in this study (Supplementary data) were performed using a Desktop 3D scanner and ScanStudio PRO ver. 1.5.2 (NextEngine, 2007). Both 360-degree and single surface scans were utilised. Macro mode was used for all specimens except for MOTA 2004.009.03, which was scanned in wide mode. Processing, alignment and fusion of scans was performed in ScanStudio PRO and saved as object files (OBJ), which were then translated to LightWave files in AccuTrans 3D V2.10.3 (MicroMouse Productions, 2007). The LightWave files were rendered in LightWave 3D 9.3 (NewTek, 2007b) to create QuickTime Virtual Reality Objects (36X36 fame QTVRs), which can be visualised and manipulated in Quicktime Mac and PC software.

The order of authors is alphabetical.

Abbreviations

Repositories: GSJ, Geological Survey of Japan, Tsukuba, Japan; KCM, Kushiro City Museum, Kushiro, Hokkaido, Japan; MOTA, Museum of the Aleutians, Unalaska, Alaska, USA; NMNS, National Museum of Nature and Science, Tokyo, Japan; UCMP, University of California Museum of Paleontology, Berkeley, California, USA; UHR, University of Hokkaido Registration, Sapporo, Japan; USNM, United States National Museum of Natural History, Washington D.C., USA.

Anatomical abbreviations: amf, anterior mental foramen; c, canine; cab, canine alveolar bulge; cf, coronoid foramen; dc, dental capsule; fc, facial crest; gi, growth increment; if, incisive foramen; lc, left canine; lpmx, left premaxilla; pms, premaxillary-maxillary suture; mc, mandibular condyle; mdf, mandibular foramen; mf, mental foramen; ml, mylohyoid line; mmf, medial mental foramen; ms, mandibular symphysis; pmf, posterior mental foramen; rpmx, right premaxilla; rmx, right maxilla; ssg, suprasymphyseal groove; sto, soft tissue outline.

Systematic paleontology

Mammalia

Desmostylia

Desmostylidae

Ounalashkastylus tomidai new genus and species

Type specimen. MOTA 2004.009.03 nearly complete left dentary with C_1, P_4 root, M_1, and M_2.

Etymology. Genus after the Aleut word *Ounalashka*, meaning 'near the peninsula', and from which *Unalaska* is derived; plus –*stylus*, Latin 'column', in reference to desmostylians. Specific name in honour of Dr. Yukimitsu Tomida, distinguished vertebrate paleontologist.

Referred specimens. USGS D848, right M^1 or M^2; MOTA 2004.009.01, incomplete left M^3; USNM 529235, natural mould of upper canines and bone fragments; MOTA 2004.009.02, natural mould of right maxilla and C^1; MOTA 2004.009.04, dorsal surface of coronoid process with M_2 and M_3; MOTA 2004.009.05, left M_1 and M_2; MOTA 2004.009.06, juvenile right dentary with dP^4; MOTA 2004.009.07, left dP^3; MOTA 2004.009.08, isolated C^1. The minimum number of individuals in this sample is four, including one neonate dentary and three specimens with M_2, all of which are considered to represent a single taxon. The three specimens with M_2 are consistent in occlusal pattern and in height of crown, as indicated qualitatively by the curvature of the crowns, and distinct from other named desmostylian taxa. Two of the specimens that have M_2 also contain M_1 and one has M_3. Non-overlapping cheek tooth remains are consistent with M_{1-3} in hypsodonty and crown curvature and inconsistent with other described desmostylians. The neonate dentary and the mould of upper tusks are referred to *Ounalashkastylus tomidai*, accepting the null hypothesis of no demonstrable taxonomic distinction in these associated specimens and no demonstrable presence of multiple desmostylian taxa. The history of the collection and description of the associated fauna was reported by Jacobs et al. (2007, 2009).

Diagnosis. Desmostylid differing from *Ashoroa* and more basal Desmostylia in having cylindrical, stylodont cusps that wear into rings of enamel surrounding exposed dentine; more derived than *Cornwallius* in having six or more cusps on lower molars; cheek teeth lower crowned (more primitive) than *Desmostylus* when compared at a similar minor stage of wear on homologous cusps and as shown by the curvature of the walls of the cylindrical cusps from the base of the crown toward the occlusal surface; less derived than *Desmostylus* and *Vanderhoofius* but similar to *Cornwallius* in that erupted M_3 does not lie in a trough developed by a medial eminence; M_3 elongate compared to *Desmostylus*.

Type locality and age. Arriaga Quarry (now the site of a school), Unalaska, Unalaska Island, Alaska. Dutch Harbor Member, Unalaska Formation. The geological setting and age were discussed by Jacobs et al. (2007) who concluded that geological and biochronological limits (excluding the evolutionary stage of *Ounalashkastylus*) lay between 24.1 and 13 Ma, but that the locality most likely falls near the Oligocene-Miocene boundary (23.03 Ma), or slightly younger.

Description

Specimens included here were initially described by Jacobs et al. (2007, 2009), prior to full preparation. We focus our descriptions here on the most informative specimens that have been fully prepared and 3D-imaged and which provide new information or modify previous work. All specimens, with measurements, are listed in Table 1.

The teeth of *Ounalashkastylus* appear less hypsodont than *Desmostylus* qualitatively because the curvature of the walls of the cylindrical cusps, especially in less worn columns, indicates proximity to the occlusal surface. A full quantitative study of hypsodonty in desmostylians is sorely needed but beyond the scope of this study. Casual examination of desmostylid cheek teeth shows that crown height varies between individuals along the tooth row, between upper and lower teeth and even among cusps on the same tooth. However, in an attempt to establish some numerical measure, we compared the height of crown in

Table 1. Measurements of specimens of *Ounalashkastylus tomidai* in millimetres. Those in parentheses are approximate.

		Measurement
	USGS D848	
Upper first or second molar	Anterior width of crown	38
Upper first or second molar	Maximum height of crown	25
	USNM 529235	
Canine (right)	Length as preserved	(161)
Canine (right)	Maximum diameter as preserved	(43)
Canine (left)	Length as preserved	(155)
Lower canine	Maximum distance between canines	(182)
Lower canine	Minimum distance between canines	(82)
	MOTA 2004.009.01	
Upper third molar	Width at the anterior row as preserved	(39)
Upper third molar	Posterior width of crown	33
Upper third molar	Maximum height of crown	(28)
	MOTA 2004.009.02	
Upper canine	Minimum diameter at the mesial end as preserved	(23)
Upper canine	Maximum diameter as preserved	(42)
Maxilla	Maximum length of maxilla as preserved	(257)
Maxilla	Maximum height of maxilla as preserved	(140)
	MOTA 2004.009.03	
Lower canine	Maximum diameter as preserved	(44)
Lower first molar	Length of crown	51
Lower first molar	Mesial width of crown	(17)
Lower first molar	Distal width of crown	(23)
Lower first molar	Maximum height of crown	19
Lower second molar	Length of crown	53
Lower second molar	Mesial width of crown	(27)
Lower second molar	Distal width of crown	(33)
Lower second molar	Maximum height of crown	31
Dentary	Maximum length of dentary as preserved	(570)
Dentary	Maximum height of dentary at coronoid process	(203)
Dentary	Height of dentary below fourth premolar	115
Dentary	Height of dentary below anterior root of first molar	118
Dentary	Height of dentary below posterior root of second molar	149
Dentary	Maximum width of dentary at symphysis as preserved	(74)
	MOTA 2004.009.04	
Lower second molar	Length of crown as preserved	(47)
Lower second molar	Mesial width of crown	(28)
Lower second molar	Distal width of crown	(27)
Lower second molar	Maximum height of crown	21
Lower third molar	Length of crown	67
Lower third molar	Mesial width of crown	40
Lower third molar	Width of poster most crown	15
Lower third molar	Maximum height of crown	33
	MOTA 2004.009.05	
Lower first molar	Distal width of crown	(33)
Lower first molar	Maximum height of crown	(25)
Lower second molar	Length of crown	58
Lower second molar	Mesial width of crown	30
Lower second molar	Distal width of crown	(34)
Lower second molar	Maximum height of crown	(25)
	MOTA 2004.009.06	
Deciduous lower fourth premolar	Length of crown	36
Deciduous lower fourth premolar	Maximum width of crown	(19)
Deciduous lower fourth premolar	Maximum height of crown	(20)
Dentary	Length of dentary as preserved	(133)
Dentary	Maximum height of dentary at coronoid process	(73)

(*Continued*)

Table 1 – *continued*

		Measurement
Dentary	Height of dentary below deciduous lower fourth premolar	(31)
Dentary	Maximum width of dentary	26
	MOTA 2004.009.07	
Deciduous upper third premolar	Length of crown	27
Deciduous upper third premolar	Mesial width of crown	(19)
Deciduous upper third premolar	Distal width of crown	21
Deciduous upper third premolar	Maximum height of crown as preserved	(9)
	MOTA 2004.009.08	
Canine	Length as preserved	(180)
Canine	Maximum diameter as preserved	(46)

the least worn cusp of upper and lower molars in the Unalaska sample with homologous, similarly worn cusps of *Desmostylus* and standardised the measure relative to tooth length in lower molars and tooth width in upper molars (because the least worn upper molar represented is a fragment that does not preserve length, MOTA 2004.009.01; described and illustrated in Jacobs et al. 2007). The least worn major lower cusp in the Unalaska sample is the posterior accessory cusp, the most posterior cusp, of M_3 in MOTA 2004.009.04 (Figure 3; cusp height = 23.3 mm; tooth length across occlusal surface = 62.8 mm). As an indication of wear, we measured the diameter of exposed dentine within the occlusal view of the cusp cylinder (dentine diameter = 2.6 mm). Analogous measurements were taken on the homologous cusp of a cast of *Desmostylus hesperus* (UCMP 32742; dentine diameter = 2.8 mm; cusp height = 28.2 mm; tooth length across occlusal surface = 54.0 mm). The ratios of cusp height to occlusal length are .371 for *Ounalashkastylus* and .522 for *Desmostylus hesperus* for these measures of the posterior accessory cusp of M_3 in these two specimens, indicating a lower crown in *Ounalashkastylus*.

For M^3, measurements of the hypocone of MOTA 2004.009.01 (tentatively identified as M^3 by Jacobs et al. 2007) are dentine diameter = 3.5 mm; cusp height = 25.0 mm; posterior width across occlusal surface = 33.6 mm. Analogous measurements on a homologous cusp were taken from a *Desmostylus* sp. M^3 (cast) from Hokkaido (KCM-AK950104) published by Kimura et al. (1998): dentine diameter = 1.8 mm; cusp height = 28.5 mm; posterior width across occlusal surface = 30.6 mm. The ratios of cusp height to occlusal width are .744 for *Ounalashkastylus* and .931 for *Desmostylus hesperus* for these measures of the hypocone of M^3 in these two specimens, again indicating a lower crown in *Ounalashkastylus*.

MOTA 2004.009.03 (Holotype; Figure 2 and 3(a); *Supplementary Material 1).*

This specimen is a nearly complete left dentary with C, posterior root of the P_4 and M_{1-2}, preserved in two blocks, the smaller being the posterior counterpart containing only a natural mould of the coronoid and parts of the two molars held in the larger block. The smaller block was moulded and scanned and the teeth digitally reconstructed. The dentary is 570 mm anteroposteriorly and lateromedially compressed due to deformation. The anterior tip of the dentary, the mandibular symphysis and the mandibular angle are damaged. No incisors or their alveoli are discernable; but the symphysis was apparently narrow. The symphysis appears to become dorsoventrally thicker and lateromedially narrower toward the anterior. The dorsal surface of the symphysis is concave dorsally, and the ventral surface ascends medially to form a dished surface (Supplementary Material 1). The posterior margin of the symphysis is 253 mm from the broken anterior margin of the mandible. A small portion of the posteroventral margin of the mandibular angle is broken away, but there is no indication of ventral expansion below the coronoid process. The mandibular notch is shallow. The mandibular condyle is damaged dorsally, posteriorly and laterally, but it was probably positioned at about the level of the occlusal surface of the M_1 and M_2. The dorsal apex of the coronoid process is broken away. However, it is low and narrow (67 mm) and slightly inflected laterally at the base, at an angle similar to the orientation of the occlusal surfaces of the teeth. The preserved anterior margin of the process is straight in lateral view. The coronoid foramen is present at the base of the process and positioned slightly medial to the process on the dorsal surface of the dentary. The mandibular foramen is shallow and positioned directly below the notch. It tapers posterodorsally towards the base of the condyle. The rounded mylohyoid line is similar to that in *Cornwallius* and extends from below the coronoid process almost to the symphysis. The submandibular fossa gradually shallows to the anterior limit of the mylohyoid line near the base of the symphysis below the anterior limit of M_1. On the lateral surface of the horizontal ramus, one mental foramen is visible anterior to the level of the preserved root of P_4. Posterior to the mental foramen, the damage has intermittently exposed the mental canal.

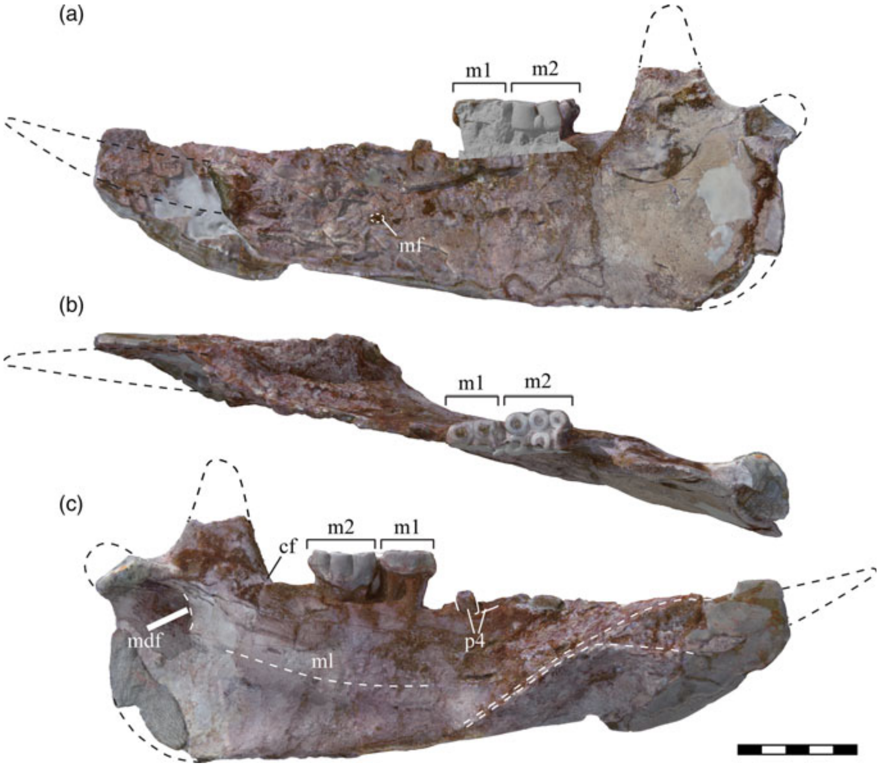

Figure 2. Left dentary (MOTA 2004.009.03) of *Ounalashkastylus tomidai*. The specimen was recovered in two blocks, the smaller holding a natural mould and portions of the teeth, here digitally reconstructed (white), in lateral (a), dorsal (b) and medial (c) views. Abbreviations: cf, coronoid foramen; mdf, mandibular foramen; mf, mental foramen; ml, mylohyoid line. Scale = 10 cm.

The dorsal surface of the alveolar margin of the dentary is slightly damaged but horizontal. The depth of the dentary is 118 mm below the anterior root of M_1 and 149 mm below the posterior root of M_2. Anterior to P_4 is a diastema of at least 259 mm. In the dorsal view, the long axis of the cheek teeth is offset anterobuccally to posterolingually from that of the dentary.

The anterolateral wall of the dentary is damaged exposing the proximal portion of the canine within the dentary. It is broken in its middle portion; the distal portion is not preserved. The canine is subcircular with a long axis running dorsoventrally in cross section, but this may be the result of the deformation after burial. The dorsoventral diameter is 44 mm at the broken midpoint ~110 mm from the anterior broken edge of the dentary and the root extends an additional 65 mm. The canine is procumbent in lateral view and directed away from the sagittal plane of the dentary.

A root for P_4 is preserved without its crown. The root is lateromedially flat with slightly excavated lateral and medial surfaces. Its diameter is 20 mm anteroposteriorly and 22 mm dorsoventrally. The alveolar margin of the dentary is damaged, but there is room for additional roots.

M_1 consists of three transverse rows of two cusps. The cusps in the buccal longitudinal row (protoconid, hypoconid and hypoconulid) are damaged buccally exposing the sagittal section and the lateral walls remain in matrix. The lingual longitudinal row comprises metaconid, entoconid and entoconid II. The distal transverse row including hypoconulid, and entoconid II, is damaged distally and is represented only by the enamel left on the posterior surface of the hypoconid and entoconid. It is not possible to identify any accessory cusps buccally and distally. In occlusal view, the size of cusps decreases posteriorly, and although the occlusal surface is damaged, the size of cusps of the distal transverse row is greatly reduced (less than 13 mm) compared to the anterior cusps because they were appressed to the anterior cusps, a result of ontogenetic restriction by M_2, which develops and erupts in *Desmostylus* anterodorsally to M_1, the tooth germ impinging on the posterior portion of that of M_2. The M_1 is lateromedially narrower than M_2. The preserved crown height is 19 mm at the metaconid. The occlusal surface of the M_1 is flat but slants down buccally. There is an interdental facet on the anterior surface of the first transverse row.

Because the lateral surface of the M_1 is damaged, it is possible to see the cross- section of its roots. The two roots are lateromedially broad. The anterior root is longer than the posterior root although the ventral margin of the anterior root is obscured because of the poor preservation. The anterior root arises from below the protoconid and metaconid. The anterior surface of the root is flat. The posterior root is located below the hypoconid and entoconid. It is narrower than the anterior root, but the posterior root is anteroposteriorly longer. The anterior and posterior roots are connected at least 13 mm below the ventral margin of the crown. Less than 1 cm of the anterior root is below the alveolar margin of the dentary; 31 mm of root are exposed above the margin.

M_2 also has three transverse rows of two cusps as seen in M_1. The tooth is rectangular in occlusal view and is less worn compared to M_1 because the crown height is greater (31 mm) and there is less lingual wear. The cusp size decreases posteriorly. The occlusal surface is concave longitudinally and transversally. There is an accessory cusp between the protoconid and hypoconid. Its apex lies at slightly more than 50% of the crown height. An accessory cusp occurs between the hypoconid and hypoconulid. It is taller and broader than other accessory cusps and almost reaches the occlusal surface. There is no wear on the cusp. The posterior surface of hypoconulid is damaged. There is no cingulum present.

The roots of M_2 are morphologically similar to those of M_1; the comparison is possible due to the damage to the lateral surface of the tooth. As seen in M_1, M_2 has two roots. The anterior root is taller and extends from the first transverse row. The posterior root is anteroposteriorly broader and appears to be fused rootlets that arise from below the second and third transverse rows (hypoconid, entconid, hypoconulid and entoconid II). The anterior and posterior roots are connected at least 8 mm below the crown-root junction.

MOTA 2004.009.04 (Figure 3(c), Supplementary Information SM2. MOTA2004.009.04.mov)

This is a left dentary fragment with M_2 and a fully erupted M_3 including a portion of the coronoid process with the coronoid foramen at its base (Jacobs et al. 2007). M_2 is composed of six cusps arranged in three ranks of two cusps each with remnants of a posterior accessory cusp (Figure 3). The tooth is broken anteriorly and labially and heavily worn, especially the labial cusps. M_3 has three ranks of two, plus two labial accessory cusps and a posterior accessory cusp. It is relatively elongate (length = 67 mm; maximum width = 40 mm; l/w = 1.7) and narrower posteriorly compared to that of *Desmostylus hesperus* (UCMP 32742; $l = 54$; $w = 41$; $l/w = 1.3$). The posterior accessory cusp is the least worn of seven major cusps. The dentary rises gently from the base of M_3 to the coronoid foramen. This is similar to the condition in *Cornwallius* but not to *Desmostylus hesperus* (UCMP 32742), the holotype of *Vanderhoofius coalingensis* (UCMP 39989), USNM 244489, which is here considered *Desmostylus*, UHR32380, the Sanjussen jaw. In those forms, the M_3 sits in a trough apparently produced by the ontogenetic posterior growth of the medial eminence. *Cornwallius* lacks a medial eminence. The remnants of the coronoid process leading to the posterior end of the tooth row indicate that the M_3 of *Ounalashkastylus tomidai* did not sit in a trough and a medial eminence was not developed.

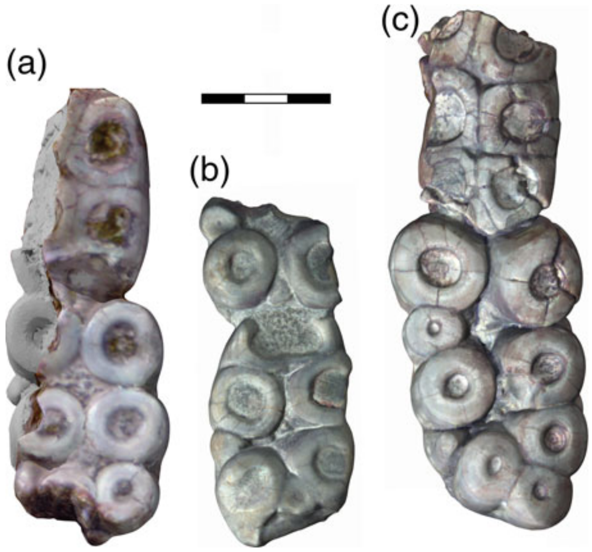

Figure 3. Lower molars of *Ounalashkastylus tomidai* in occlusal view: (a) MOTA 2004.0009.03, left M_{1-2}, buccal portions of protoconid, hypoconid and accessory cusp digitally reconstructed from natural mould; (b) MOTA 2004.0009.05, left M_{1-2}; (c) MOTA 2004.0009.04, left M_{2-3}. Scale = 3 cm.

*USNM 529235 (*Figure 4*).*

This specimen is a mould of a rostrum with two tusks. Remnants of enamel adhere to the tusk moulds and bone fragments extend between them. Bone is missing in an anteroposteriorly elongate ellipsoid incisive foramen (43 mm × 7 mm), located anterior to the root of the canine. The maximum bone thickness at the posterior transverse break is 3 mm on both the right and left premaxillaries. The premaxillaries together are concave ventrally indicating a vaulted palate. The left tusk is 161 mm long, and the right tusk is 155 mm long. The maximum diameter of the left tusk is 43 mm, and that of the left tusk cannot be measured because of the poorly preserved lateral surface of the tusk. The maximum distance between the medial surfaces of the two tusks is 182 mm at the tip, and the minimum distance is 82 mm between the bases. The two tusks are directed laterally away from the sagittal plane of the skull, but probably close to their natural position. The tusks show a number of shallow transverse grooves representing growth increments. No alveoli for incisors are preserved in this natural mould.

Preservation of the Unalaska specimens often leaves red halos around the bone. Jacobs et al. (2007, their

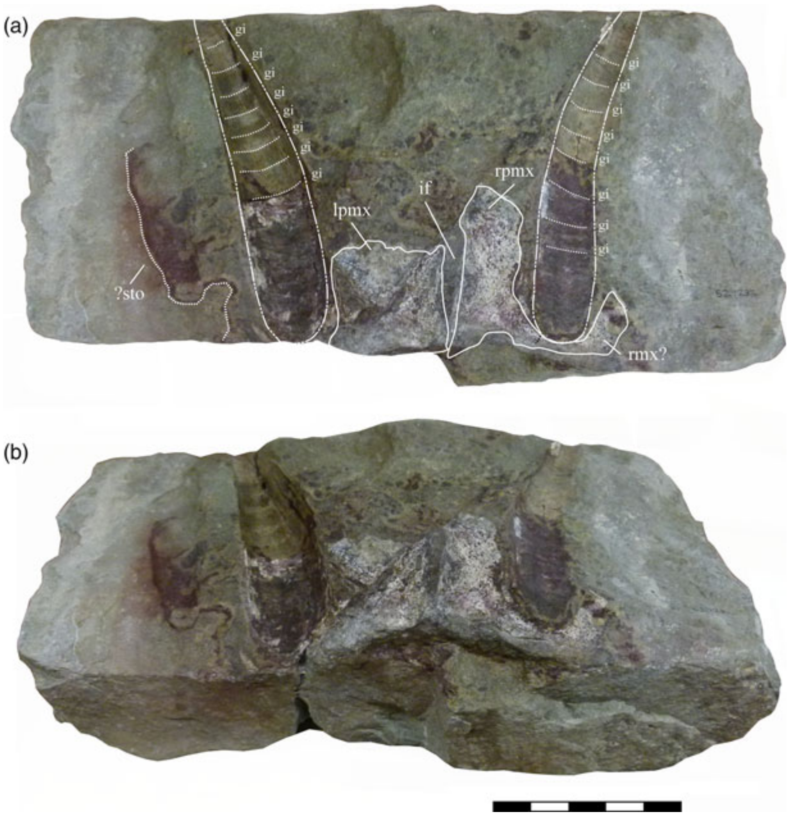

Figure 4. Natural mould of rostrum with tusk impressions and remnants of bone (USNM 529235) of *Ounalashkastylus tomidai* in dorsal view (a) and in oblique view (b). USNM 529235 shows red staining from the right maxilla, along the palate, lateral to the left premaxilla, in the speculated position of snout soft tissue.

Figure 2) illustrated MOTA 2004.009.04 prior to completion of preparation, showing a circular mineralogical ghost of a presumed upper molar column over a lower tooth, as if in occlusion. The staining is clearly associated with and mediated by fossils, not randomly distributed throughout the matrix, suggesting conditions of fossilisation capable of preserving remnants of missing tissue as geochemical residues. In USNM 529235, iron staining occurs on the matrix of the tusk moulds consistent with a biogenic cause. It follows the bone beginning 16 mm lateral to the right maxilla, then along the oral surface of the palate. From the palate the halo can be traced continuously past the area of left maxilla where it folds on itself at a distance of 39 mm from the canine. We speculate that in this instance it possibly reflects soft tissue associated in life with the snout.

*MOTA 2004.009.02 (*Figure 5*).*

This is a natural mould of a right maxilla with patchy adherent bone and fragments of the tusk preserved. As preserved, the dorsal margin of the maxilla is gently convex upwards. The lateral wall bulges from the base of the tusk towards the dorsomedial margin, where the bulge flattens. The posteroventral portion of the mould indicates a discrete but rounded and curved bulge anterior to the orbit and infraorbital foramen. In *Cornwallius*, these are referred to as the canine alveolar bulge and facial crest by Beatty (2009). Along the posterodorsal margin, a small linear trough marks an offset in orientation along what we take to be the maxillary–premaxillary suture. This interpretation is consistent with the orientation of the tusk, which in other taxa follows the dorsal margin of the maxilla.

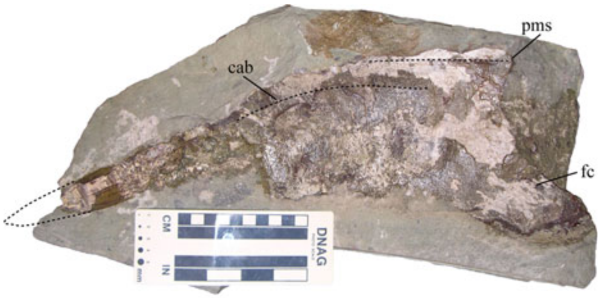

Figure 5. Natural mould of the right maxilla with adherent bone and tusk (MOTA 2004.009.02) of *Ounalashkastylus tomidai*.

The tip of the tusk is broken away showing a dorsoventrally elongate, oval cross section. At the distal broken surface the diameter is 23 mm, and tooth enamel is 2 mm thick. Posteriorly, the diameter increases to 32 mm, which is measured 39 mm from the preserved distal tip of the tusk. The proximal end of the tusk is hard to determine because the proximal region is poorly preserved and represented only by fragments of dentine and an ambiguous outline at ~137 mm from the preserved distal margin of the tusk. The tusk is elongate, straight from its base and forwardly directed. There is no evidence of cheek teeth and the ventral margin of the maxilla is broken away.

Dental formula of Ounalashkastylus tomidai.

Jacobs et al. (2007) described, illustrated and discussed morphological variation among cheek teeth and assigned tooth positions of known specimens of *Ounalashkastylus tomidai*, here shown for lower molars in Figure 3 (see also Supplemental Material). Preparation and examination of specimens allows revision of the preliminary conclusions expressed previously. Available specimens do not provide definitive evidence of the presence of incisors. Canine tusks are present in both upper and lower jaws. A juvenile or neonate right dentary, split sagitally, shows an erupting tooth with seven cusps (two ranks of three plus a posterior median cusp), and there is no room below it to house a replacement tooth (MOTA 2004.009.06; Fig. 10 of Jacobs et al., 2007, and Figure 2 of Jacobs et al. 2009; Supplementary Material). An additional tooth is forming posterior to it, and a small tooth root is well anterior to it. The erupting tooth resembles dP_4 in *Desmostylus*, and it is small compared the M_1 of *Ounalashkastylus* (width ~18 mm, length ~40 mm, compared to width of broken M1 of holotype of ~24 mm, which misses approximately a third of its width, and length of ~46 mm). The anterior tooth root probably belonged to a deciduous premolar lost early in life, probably dP_2 because the intervening space anterior to dP_4 must represent an alveolus for dP_3. However, the premolar formula is uncertain. Our current inference of the dental formula of *Ounalashkastylus* is $I^{?}/_{?}$, $C^{1}/_{1}$, $(d)P^{?}/_{3}$, $M^{3}/_{3}$.

Description of the Sanjussen jaw

The Sanjussen jaw (UHR32380; Figure 6) was discovered in situ in the Middle Miocene, marine Chikubetsu Formation (Hashimoto et al. 1965; Koma et al. 1974; Kurita et al. 1992; Figure 1). The specimen was excavated from pebbly sandstone with abundant allochthonous bivalve shells. It is a very large dentary, nearly complete from the symphysis to the mandibular condyle, missing some pieces. The anterior portion of the symphysis is damaged and the coronoid process was not preserved. The lateral surface has gaps, but the surface is constrained by the surrounding wall. A portion of the ventral margin of the horizontal ramus is broken away anterior to the posterior mental foramen. The dental capsule is large and continuous with a medial swelling to form a medial eminence along the myohyoid line that extends anteriorly to the posterior portion of the mandibular symphysis. The dorsal surface of the dental capsule is damaged. Four posterior columns from the broken M_2 and two anterior columns from M_3 are present.

The most conspicuous feature of the lower jaw is the protuberant, elongate, rounded medial eminence, which rises dorsally to the level of the occlusal surface of the M_2 and reduces the volume of the suprasymphysial groove. The eminence has a smooth surface with constrictions running perpendicular to the long axis of the body. In posterior view (Figure 6(f)) it appears almost shelf-like at the dental capsule, but becomes more cylindrical and is gently curved anteriorly. The medial eminence is composed of dense trabecular bone and does not appear to be pathological because of (1) the uninterrupted structural consistency in the CT data (Figure 6(g)) and (2) the presentation of the medial eminence occurs in some other desmostylid specimens, although morphology varies, for example *D. hesperus* (UCMP 32742) and *V. coalingensis* (UCMP 39989) from California have a ventrally convex medial margin of the medial eminence.

The mandibular symphysis exceeds half the length of the mandible. It is slightly convex in the lateral view and ascends at an angle of approximately 25° to the occlusal plane. The mandibular symphysis is fused as indicated by the rugose texture along the suture. The suture line would intersect the lateral surface of the dentary at an angle of 20° in dorsal and ventral views, suggesting the fused dentaries converged towards the midline (Figure 6(a)), similar to *V. coalingensis* but unlike *D. hesperus*. The suprasymphysial depression is extremely narrow and diminishes anteriorly because of the eminence.

The anterior tip of the mandible is nearly quadrate in cross section. The diastema is long extending two-thirds the preserved length of the mandible. A paraglossal crest is not preserved (Yoshiwara and Iwaski 1902; Reinhart 1959). A large tusk is far lateral, indicating that it is a canine (Uno and Kimura 2004). The preserved length of the canine is 325 mm in dorsal view and its diameter is 60 mm (Figure 6(a) and (e)). A mental canal (diameter = 25 mm), visible due to breakage, bifurcates, leading to the anterior and middle mental foramina. The middle mental foramen (aperture = 13 mm) is located on the anteroventral side of the mandible. The posterior mental foramen is obscure due to breakage but exhibits a slight depression on the lateral side of the mandibular body.

The ascending ramus is flat and thin. The thickness is consistent from the ascending ramus to the neck of mandibular condyle. The mandibular condyle has an

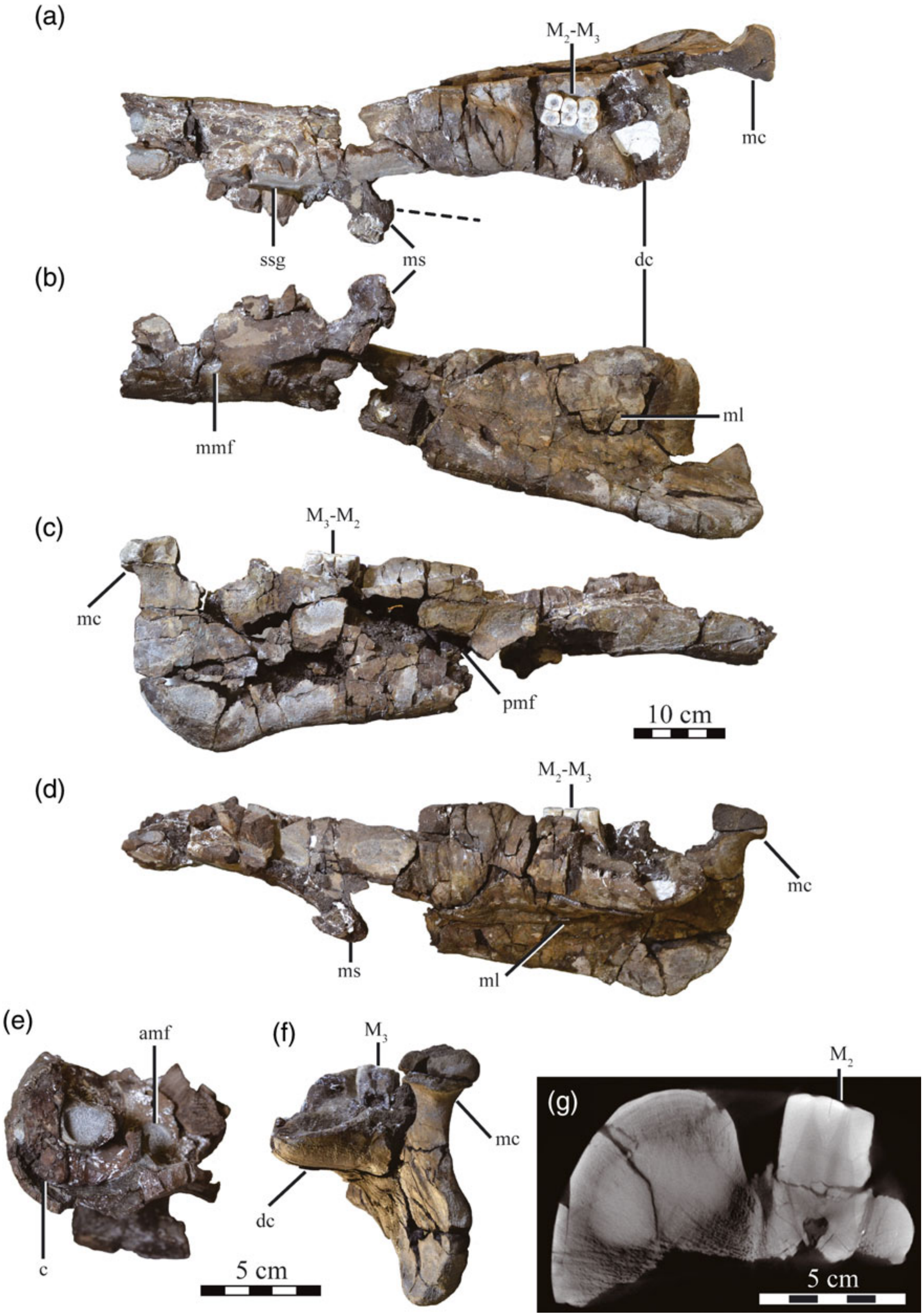

Figure 6. Sanjussen specimen, cf. *Vanderhoofius* sp. (UHR32380), in (a) dorsal view; (b) ventral view; (c) lateral view; (d) medial view; (e) anterior view; (f) posterior view and (g) micro-CT image at the posterior part of the mandible. Dotted line indicates the midline suggested by fused suture. Abbreviations: amf, anterior mental foramen; c, canine; dc, dental capsule; mc, mandibular condyle; ms, mandibular symphysis; pmf, posterior mental foramen; ssg, suprasymphyseal groove.

obvious neck and is slightly higher than the occlusal surface of the teeth. The articular surface of the condyle is eroded but convex and inclined posteriorly at an angle of 45° to the occlussal surface. A mandibular foramen is located on the medial side of the neck of the mandibular condyle. The ventral half of the mandibular body thickens gradually from the angle of the ascending ramus.

Two partial molars are identified as M_2 and M_3 because UHR 32380 has no premolars and premolars are lost after M_1 is shed in *Desmostylus* (Inuzuka 1988). The two molars are hypsodont and stylodont with short roots. The anterior two columns of M_2 are missing but the posterior four columns, which are assigned to hypoconid, entoconid, hypoconulid and entoconid II, are present. The anterior two columns, protoconid and metaconid, of M_3 are preserved. No extra cuspids or cingula are present. Based on the preserved roots, M_2 length = 590 mm, width = 316 mm; M_3 length = 615 mm, width = 364 mm. Appression facets of adjacent margins indicate the two molars were packed tightly. The M_2 (crown height = 30.5 mm from CT data) is worn more than the M_3 (crown height = 34.4 mm from CT data). We refer the Sanjussen specimen to cf. *Vanderhoofius* sp. because the symphysis is dorsoventrally thin, it lacks incisors with a resultant tapering of the anterior half of the horizontal ramus, and the presence of the medial eminence anterior to M_2. This is the first record of *Vanderhoofius* in the western North Pacific realm.

Ontogeny of the dentary and its taxonomic implications

To assess ontogenetic variation related to expansion of the medial eminence quantitatively, dentary length, dentary width, molar lengths and canine diameter of the Sanjussen specimen were compared with those of *Desmostylus* and *Vanderhoofius* specimens having well developed medial eminences (Figures 7 and 8). Specimens that have shed M_1 are consistently larger and presumably more mature than those specimens that retain M_1 (Inuzuka 1988). Mandibular width, which reflects the prominence of the medial eminence, increases in specimens lacking M_1. In smaller specimens with only M_1 and M_2 erupted, the medial eminence is not observed except as dental capsules (Uno and Kimura 2004). In medium-sized individuals with M_2–M_3 erupted, the medial eminence extends anteriorly and posteriorly but is less developed in the middle portion of the dentary. In larger specimens (UCMP 32742), a distinct constriction lies between the anterior and posterior portions of the eminence. In the Sanjussen dentary, the eminence develops along the entire length of the mandibular body and the width of the mandibular body is consistent in the dorsal view.

Canine width appears to increase as individuals increase in gross size and apparently shed incisors with

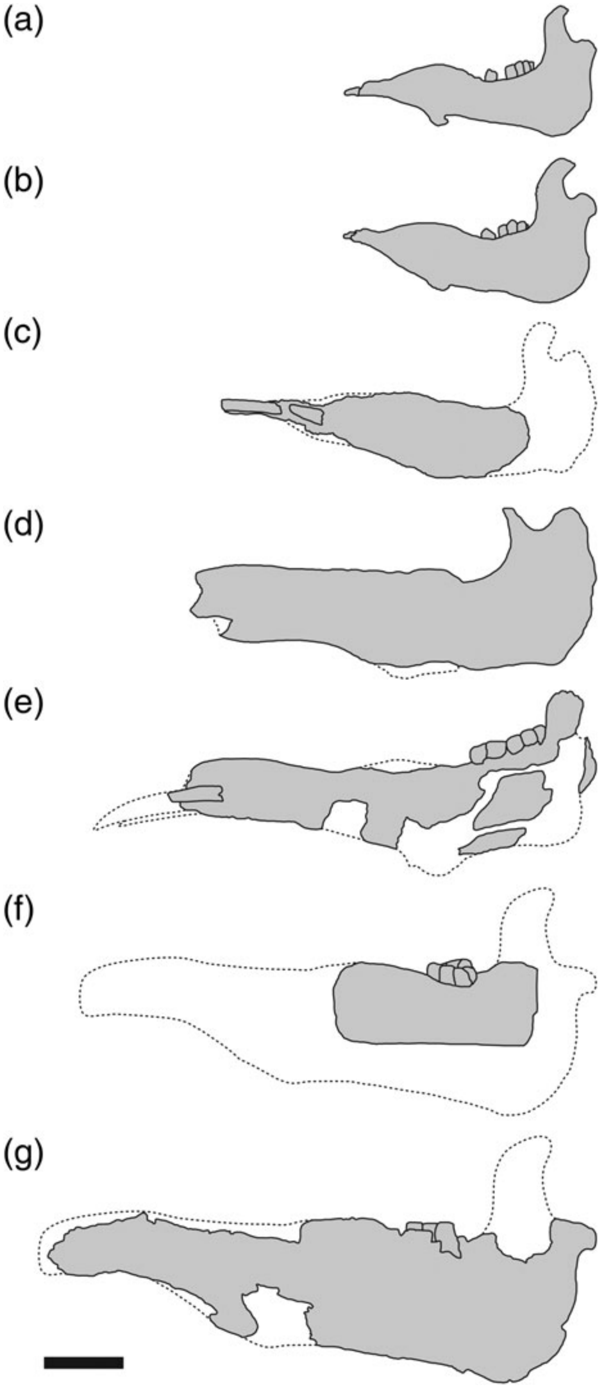

Figure 7. Size comparison of desmostylid mandibles: (a) *Desmostylus hesperus* (based on GSJ-F07745; Uno and Kimura, 2004); (b) *D. hesperus* (based on GSJ-F07743; Inuzuka, 1988); (c) *D. japonicus* (based on NSM-PV5600; Kohno, 2000); (d) *Vanderhoofius coalingensis* (based on UCMP39989; Reinhart, 1959); (e) *D. hesperus* (based on UCMP32742; Reinhart, 1959); (f) *D.* sp. (GSJ-F02071; Tokunaga, 1936); (g) Sanjussen specimen (UHR32380). Note that the Sanjussen specimen is the largest among the known desmostylid specimens. Scale = 10 cm.

age. Upper incisors of *Desmostylus* and *Cornwallius* were suggested to be absent or deciduous (Kohno 2000; Beatty 2009), but lower incisors were present and thought to be erupting in a medial-to-lateral direction in *Desmostylus* (Kohno 2000). The sample size examined here is small; however, the loss of lower incisors in *Vanderhoofius*, which has large canines, compared to the retention of lower incisors along with large canines in *D. hesperus*, is a character that may support the distinct taxonomic status of *Vanderhoofius* because they do not follow simple size increase (Figure 8). Therefore, we tentatively refer the Sanjussen specimen to cf. *Vanderhoofius* sp.

Phylogenetic analysis

In order to assess phylogenetic relationships of *Ounalashkastylus tomidai* and the Sanjussen specimen within Desmostylia, we used a matrix of 37 characters from Beatty (2009) and two newly added characters (character 38: number of major cusps on M$_2$ less than 6 (0), equal to or more than 6 (1); character 39: number of major cusps on M$_3$ less than 7 (0), equal to or more than 7 (1)). The holotype of *Ounalashkstylus tomidai* and the referred specimens are coded as a single operational taxonomic unit (OTU). We also added Anthracobunidae as an outgroup taxon because anthracobunids were suggested to be a sister clade to Desmostylia by Delmer (2009) and Cooper et al. (2014). The character states of Anthracobunidae were coded as an OTU based on multiple anthracobunid specimens and taxa described in Cooper et al. (2014). The character states of pachyosteosclerosis in the postcranial skeleton (character 20) were modified following Hayashi et al. (2013). All characters in this analysis were unordered. The phylogenetic analysis was conducted in PAUP* 4.0a142 (Swofford 2002) using a branch and bound tree search with ACCTRAN character optimisation. Twelve parsimonious trees were obtained (tree length = 60, consistency index = 0.70, retention index = 0.76, rescaled consistency index = 0.53). In the topology of the strict consensus tree (Figure 9), the relationship between outgroup taxa and ingroup (Desmostylia) was not resolved as seen in Cooper et al. (2014). The strict consensus tree (Figure 9) shows *Ounalashkastylus tomidai* in a clade with *Desmostylus, Vanderhoofius* and the Sanjussen specimen, supported by three unambiguous synapomorphies, character 15 (extra cusps on molars are large and approaching the size of main cusps), and 38 and 39, both relating to increased number of cusps. Note that *Ounalashkastylus tomidai* has an unambiguous autapomorphy (character 27, the cross-sectional shape of the lower canine is medio-laterally compressed) and this new taxon is more derived than *Cornwallius* and the sister taxon to the clade including *Desmostylus, Vanderhoofius and* the Sanjussen desmostylid. The Sanjussen desmostylid is in an unresolved polytomy with *Desmostylus* and *Vanderhoofius*; therefore, this analysis as represented by the strict consensus tree neither supports nor rejects the taxonomic assignment of the Sanjussen specimen to *Vanderhoofius*, although the absence of incisors (character 16) is an ambiguous synapomorphy of a clade comprising

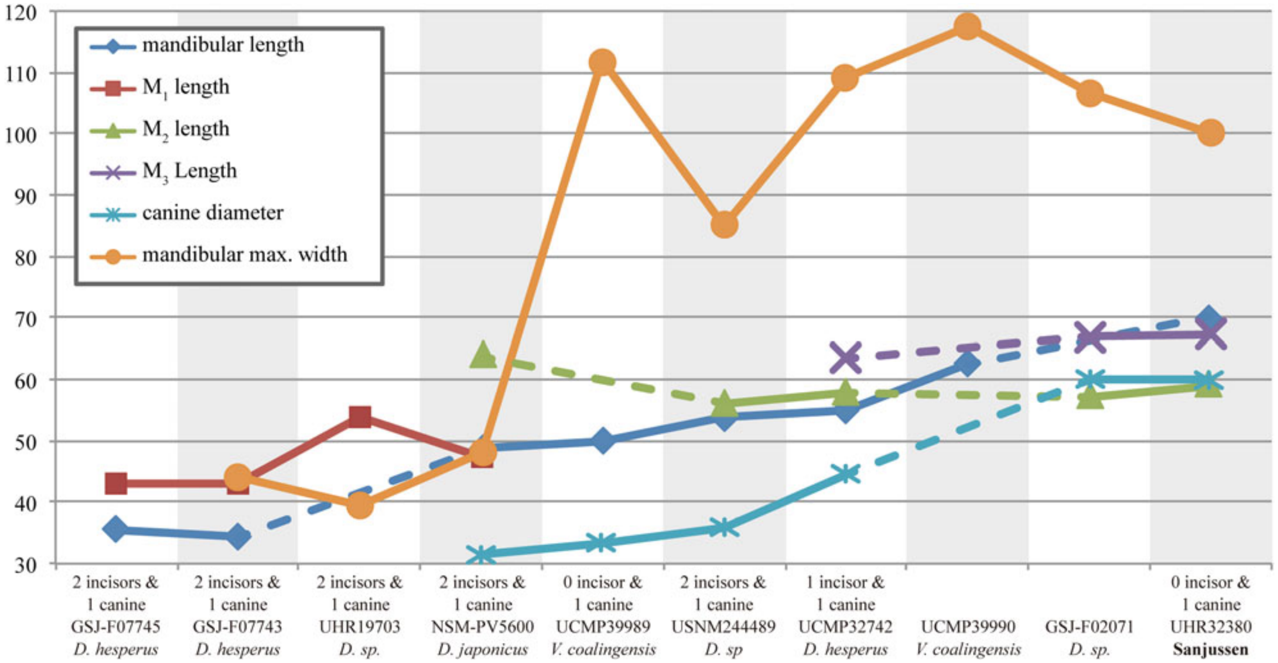

Figure 8. Ontogenetic comparisons of mandibular measurements and characters among *Desmostylus* and *Vanderhoofius*. The unit is centimetre for mandibular length and millimetre for the others.

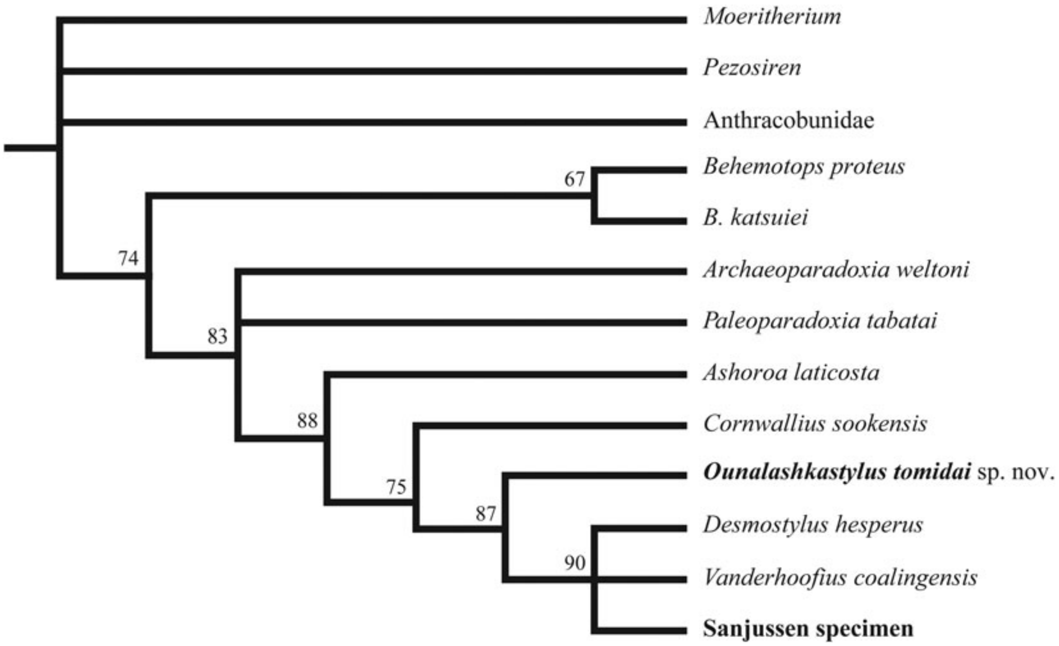

Figure 9. Strict consensus tree showing *Ounalashkastylus tomidai* as more derived than *Cornwallius* and the sister taxon to the clade including *Desmostylus, Vanderhoofius* and the Sanjussen desmostylid.

the Sanjussen desmostylid and *Vanderhoofius* in four of the 12 most parsimonious trees. This clade including *Desmostylus, Vanderhoofius and* the Sanjussen desmostylid is supported by three unambiguous synapomorphies: M_2 without extra cupsid (character 10), swelling of the mandible (character 24), loss of upper canine (character 26).

Discussion and conclusions

In our phylogenetic analysis, *Cornwallius*, *Ounalashkastylus* and *Desmostylus* plus *Vanderhoofius* constitute an informative sequence of character acquisition in this enigmatic order of mammals. *Cornwallius* heralds the attainment of true stylodonty in desmostylids and, as *Cornwallius* is represented by very good skull specimens, it also heralds the acquisition of a vaulted palate and elongate snout within the family. *Ounalashkastylus*, with its intermediate height of crown, derived number of tooth columns, but apparent lack of hypertrophied medial eminence, falls between *Cornwallius* and *Desmostylus*, specifically demonstrating the evolutionary addition of supernumerary columns in teeth prior to the development of the medial eminence. Both of these characters relate to feeding, the supernumerary columns as tooth components and the medial eminence as attachment for mylohyoid musculature or its modification.

The vaulted palate in desmostylids has been suggested to facilitate suction feeding (Beatty 2004; Uno et al. 2008). In this case, the cheek teeth may have been kept clinched, acting as buttresses to hold the jaws tight while the piston action of the tongue and hyoid muscles generated the negative pressure necessary for suction feeding. The elongate jaws and expanded facial region would, in that case, facilitate extensive adductor, facial, pterygoid and hyoid musculature necessary for such a method of feeding. The red halo along the anterior region of the skull in *Ounalashkastylus tomidai* (USNM 529235) may provide a crude suggestion of the soft tissue outline of the snout.

During the evolution of more derived taxa, the enhancement of the medial eminence may have seated hyoid and pterygoid musculature and strengthened the brace of the molars in suction feeding especially in larger and older individuals. In addition, the medial eminence of the horizontal ramus would have provided a seat of origin for huge mylohyoid muscles, which would have reinforced the floor of the oral cavity and functioned with the hyoids to produce powerful swallowing forces.

An extremely well developed medial eminence is seen only in *Desmostylus* and *Vanderhoofius* (Figure 8). The increased volume and relatively dense internal structure adds weight to the head of these animals. While the postcrania of *Desmostylus* exhibits more spongy inner microstructure than some other members in Desmostylia (Hayashi et al. 2013), the dense medial eminence of adults in this clade appears synapomorphic and to have functional significance for bottom feeding by decreasing the buoyancy of the head relative to the body. A similar condition and interpretation has been proposed for extant walruses (*Odobenus*) and for the fossil walrus-like odontocete cetacean *Odobenocetops* (Kaiser 1970; de Muizon et al. 2002). In addition, *Odobenocetops* and walruses have robust paroccipital processes, as do desmostylids (Inuzuka 2000). In walruses these processes support strong neck muscles used in bottom feeding (Kastelein and Gerrits 1990) and the same is inferred for *Odobenocetops* (de Muizon et al. 2002), and here presumed the same for *Desmostylus* and *Vanderhoofius*. Neither the heavy skull nor spongy postcrania occur in *Paleoparadoxia*. Therefore, these morphological differences between *Paleoparadoxia* and *Desmostylus* may suggest a difference in feeding behaviour, which can be related to habitat differences suggested in Hayashi et al. (2013).

Generally, the morphological uniqueness and variability of desmostylid molars and the lack of consistent functional patterns of wear analogous to other mammals suggest minimal food processing and renders the interpretation of their diet from tooth morphology extremely difficult. While the teeth, inferred ingestion mechanism and hypothesised behaviour do not specifically limit the preferred diet, stable isotope values do. Clementz et al. (2003) utilised carbon, oxygen and strontium isotopes to infer the life habits of *Desmostylus*. They concluded that the specimens they analysed represented an aquatic herbivore that foraged in estuarine and coastal freshwater systems. We attempted to test their conclusions regarding desmostylians by determining δ^{13}C and δ^{18}O values for enamel of *Ounalashkastylus* and its entombing matrix. The negative values of the enamel ($\delta^{13}C = -6.25$; $\delta^{18}O = -20.92$) and matrix ($\delta^{13}C = -7.20$; $\delta^{18}O = -29.44$), indicate exchange with groundwater, consistent with the conclusions of Perfit and Lawrence (1979), who determined meteoric waters had interacted with the nearby Captains Bay Pluton affecting isotope values (Jacobs et al. 2007).

However, in addition to the stable isotope data of Clementz et al. (2003), the morphology of the teeth in basal desmostylians as well as their closest outgroup, whether afrotherian or *Anthracobune*, support a herbivorous diet (Domning 2008). This, and their consistent occurrence in coastal deposits, suggest shallow feeding on marine algae, sea grass or other near shore plants. Accepting a sister relationship between Desmostylia and Asian anthracobunids as discussed by Cooper et al. (2014), desmostylians are an independently evolved group of marine herbivores, not sister to Sirenia, their competitors (Domning 2008), but convergent in diet.

Acknowledgements

It is our great pleasure to honour our friend, colleague, fellow student and mentor, Dr. Yukimitsu Tomida, with this contribution to the understanding of desmostylids, a group of fossil mammals important in Japan and the United States, the two countries that have produced most of their fossils. We thank the Museum of the Aleutians in Unalaska for facilitating the loan of Alaskan material for our study. We thank Dr. David Norton for his participation in the field component in Alaska as well as his role in facilitating our introductions to the Unalaska community. Preparation of the fossil material from the Museum of the Aleutians was performed at the Perot Museum of Nature and Science directed by Dr. Ronald Tykoski and at SMU by Kent Newman. We thank the crew (Atsushi Kurosawa, Takuma Nishi, Daisuke Aihara) from the lab of Dr. Nachio Minoura, former professor in Hokkaido University Museum, who excavated the Sanjussen specimen. We thank Dr. Makoto Manabe for permission to use the micro-CT scanner at the National Museum of Nature and Science, Tokyo. We thank Dr. Ryoko Matsumoto and Chisako Sakata for operation of the micro-CT scanner and members of Dr. David Evans' lab (University of Toronto) for discussion and Dr. Hiroshi Sawamura for his hospitality and helpfulness at the Ashoro Museum, Japan. We thank David Bohaska (USNM) for his help. Kurt Ferguson of SMU determined stable isotope values from Unalaska. LLJ benefitted from Dr. Anthony Fiorillo who facilitated his inclusion in the Alaska field programme and a Visiting Professorship at Hokkaido University Museum, providing affiliation in Japan with Dr. Yoshitsugu Kobayashi and his students (KC, KT). Time spent with them provided a broader opportunity, helped define this study and facilitated an important intellectual friendship with Dr. Naoki Kohno. LLJ's recent students (Y Kimura and YN) are important contributors to this paper. Portions of this research were addressed in an MS thesis by YN directed by LLJ at SMU and funded by the Institute for the Study of Earth and Man. We thank Drs. Nicholas Pyenson and David Bohaska for access to specimens at the USNM and Dr. Pat Holroyd at the UCMP. We are grateful for improvements to the manuscript facilitated by an anonymous reviewer.

Disclosure statement

No potential conflict of interest was reported by the authors.

Funding

Fieldwork was supported by grants from the Alaska Region, US National Park Service, to ARF, and the Institute for the Study of Earth and Man to LLJ.

Supplemental data

Supplemental data for this article can be accessed here: 10.1080/08912963.2015.1046718

References

Barnes LG. 2013. A new genus and species of late Miocene paleoparadoxiid (Mammalia, Desmostylia) from California. Los Angeles County Museum Contributions in Science. 521:51–114.

Beatty BL. 2004. Evidence for suction feeding in the Desmostylidae (Desmostylia, Mammalia). J Morphol. 260:276–277.

Beatty BL. 2009. New material of *Cornwallius sookensis* (Mammalia: Desmostylia) from the Yaquina Formation of Oregon. J Vert Paleontol. 29:894–909. doi:10.1671/039.029.0320.

Clementz MT, Hoppe KA, Koch PL. 2003. A paleoecological paradox: the habitat and dietary preferences of the extinct tethythere *Desmostylus*, inferred from stable isotope analysis. Paleobiology.

29:506–519. doi:10.1666/0094-8373(2003)029<0506:APPTHA>2.0.CO;2

Cooper LN, Seiffert ER, Clementz M, Madar SI, Bajpai S, Hussain ST, Thewissen JGM. 2014. Anthracobunids from the Middle Eocene of India and Pakistan are stem perissodactyls. PLoS ONE. 9:e109232. doi:10.1371/journal.pone.0109232.

de Muizon C, Domning DP, Ketten DR. 2002. *Odobenocetops peruvianus*, the walrus-convergent delphinoid (Mammalia: Cetacea) from the Early Pliocene of Peru. Smithsonian Contributions to Paleobiology. 93:223–261.

Domning DP. 2001. Evolution of the Sirenia and Desmostylia. In: Mazin J-L, de Buffrénil V, editors. Secondary Adaptation of Tetrapods to Life in Water. München: Verlag Dr. Dr. Friedrich Pfeil; p. 151–168.

Delmer C. 2009. Reassessment of the generic attribution of *Numidotherium* savagei and the homologies of lower incisors in proboscideans. Acta Palaeontol Pol. 54:561–580. doi:10.4202/app.2007.0036.

Domning DP. 2002. The terrestrial posture of desmostylians. Smithsonian Contributions to Paleobiology. 93:99–111.

Domning DP. 2008. Desmostylia. In: Janis CM, Gunnell GF, Uhen MD, editors. Evolution of Tertiary Mammals of North America. Cambridge: Cambridge University Press; p. 639–644.

Domning DP, Pyenson ND. 2008. “Snagging” teeth and premolar homologies in Paleoparadoxiidae (Mammalia: Desmostylia). J Vert Paleontol. 28:923–927. doi:10.1671/0272-4634(2008)28[923:STAPHI]2.0.CO;2.

Gingerich P. 2005. Aquatic adaptation and swimming mode inferred from skeletal proportions in the Miocene desmostylian *Desmostylus*. J Mamm Evol. 12:183–194. doi:10.1007/s10914-005-5719-1.

Hashimoto W, Nagao S, Kanno S. 1965. Explanatory text of the geological map of Japan, 1: 50,000, Soeushinai. Sapporo: Hokkaido Development Agency.

Hayashi S, Houssaye A, Nakajima Y, Chiba K, Ando T, Sawamura H, Inuzuka N, Kaneko N, Osaki T. 2013. Bone inner structure suggests increasing aquatic adaptations in Desmostylia (Mammalia, Afrotheria). PLoS ONE. 8:e59146. doi:10.1371/journal.pone.0059146.

Inuzuka N. 1988. The skeleton of *Desmostylus* from Utanobori, Hokkaido, I. Cranium. Bull Geol Survey Jpn. 39:139–190.

Inuzuka N. 2000. Primitive Late Oligocene desmostylians from Japan and Phylogeny of the Desmostylia. Bull Ashoro Museum Paleontol. 1: 91–123.

Jacobs LL, Fiorillo AR, Gangloff R, Pasch A. 2007. Desmostylian remains from Unalaska Island, Aleutian Chain, Alaska. Bull Carnegie Mus Natl History. 39:189–202. doi:10.2992/0145-9058(2007)39[189:DRFUIA]2.0.CO;2.

Jacobs LL, Fiorillo AR, Nishida Y, Fitzgerald EMG. 2009. Mid-Cenozoic marine mammals from Alaska. In: Albright LB III, editor. Papers on Geology, Vertebrate Paleontology, and Biostratigraphy in honor of Michael O Woodburne. Bull Mus Northern Arizona. 65:171–184.

Kaiser HE. 1970. Comparative studies on the bone structure of the Pinnipedia: structure of the skull of the walrus, *Odobenus rosmarus* L. Anat Anz. 127:1–21.

Kastelein RA, Gerrits NM. 1990. The anatomy of the walrus head (*Odobenus rosmarus*): Part 1. The skull. Aquat Mamm. 16:101–119.

Kimura M, Yahata M, Sawamura H, Segawa I, Suzuki A, Muraishi Y. 1998. The vertebrate fossils and their horizon from Akan-Cho. Eastern Hokkaido, Japan. Earth Sci. (Chikyu Kagaku) 52:44–50.

Kohno N. 2000. A centenary of studies on the holotype (SM-PV 5600) of *Desmostylus japonicus* Tokunaga and Iwasaki, 1914. Bull Ashoro Mus Paleontol. 1:137–151.

Koma T, Ito S, Yokota S, Kamishima H. 1974. Chemical composition of Neogene muddy rocks from Chikubetsu area, northwestern Hokkaido, Japan. J Japan Assoc Pet Tech. 39:95–105.

Kurita H, Ichinoseki T, Hiramatsu C. 1992. Geologic age of the Sankebetsu and Haboro Formations, Haboro area, northern Hokkaido. J Geol Soc Japan. 98:259–266.

Perfit MR, Lawrence JR. 1979. Oxygen isotopic evidence for meteoric water interaction with the Captains Bay Pluton, Aleutian Islands. Earth Planetary Sci Lett. 45:16–22. doi:10.1016/0012-821X(79)90103-1.

Reinhart RH. 1959. A review of the Sirenia and Desmostylia. Univ California Publ Geol Sci. 16:1–146.

Tokunaga S. 1936. *Desmostylus* found near the town of Yumoto, Fukushima Prefecture. J Geogr. 48:473–484. doi:10.5026/jgeography.48.473.

Swofford DL. 2002. PAUP*. Phylogenetic Analysis Using Parsimony (*and Other Methods). Version 4. Sinauer Associates, Sunderland, Massachusetts.

Uno H, Kimura M. 2004. Reinterpretation of some cranial structures of *Desmostylus hesperus* (Mammalia: Desmostylia): a new specimen from the Middle Miocene Tachikaraushinai Formation, Hokkaido, Japan. Paleontol Res. 8(1):1–10. doi:10.2517/prpsj.8.1.

Uno H, Yoneda M, Taru H, Kohno N. 2008. Dietary preferences of desmostylians based on isotope, microwear and cranial morphology. J Vert Paleontol. 28:155A.

Yoshiwara S, Iwaski J. 1902. Notes on a new fossil mammal. J College Sci Imperial Univ Tokyo. 16:1–13.